



HHS Public Access

Author manuscript

Small. 2016 July ; 12(28): 3861–3869. doi:10.1002/sml.201600737.

Published in final edited form as:

Small. 2016 July ; 12(28): 3861–3869. doi:10.1002/sml.201600737.

On-Chip Production of Size-Controllable Liquid Metal Microdroplets Using Acoustic Waves

Dr. Shi-Yang Tang,

Department of Engineering Science and Mechanics, The Pennsylvania State University, University Park, PA 16802, USA

Bugra Ayan,

Department of Engineering Science and Mechanics, The Pennsylvania State University, University Park, PA 16802, USA

Nitesh Nama,

Department of Engineering Science and Mechanics, The Pennsylvania State University, University Park, PA 16802, USA

Dr. Yusheng Bian,

Department of Engineering Science and Mechanics, The Pennsylvania State University, University Park, PA 16802, USA

Dr. James P. Lata,

Department of Engineering Science and Mechanics, The Pennsylvania State University, University Park, PA 16802, USA

Prof. Xiasheng Guo, and

Department of Engineering Science and Mechanics, The Pennsylvania State University, University Park, PA 16802, USA; Key Laboratory of Modern Acoustics (MOE) Department of Physics Nanjing University, Nanjing 210093, China

Prof. Tony Jun Huang

Department of Engineering Science and Mechanics, The Pennsylvania State University, University Park, PA 16802, USA

Abstract

Micro- to nanosized droplets of liquid metals, such as eutectic gallium indium (EGaIn) and Galinstan, have been used for developing a variety of applications in flexible electronics, sensors, catalysts, and drug delivery systems. Currently used methods for producing micro- to nanosized droplets of such liquid metals possess one or several drawbacks, including the lack in ability to control the size of the produced droplets, mass produce droplets, produce smaller droplet sizes, and miniaturize the system. Here, a novel method is introduced using acoustic wave-induced forces for on-chip production of EGaIn liquid-metal microdroplets with controllable size. The size distribution of liquid metal microdroplets is tuned by controlling the interfacial tension of the

Supporting Information

Supporting Information is available from the Wiley Online Library or from the author.

metal using either electrochemistry or electrocapillarity in the acoustic field. The developed platform is then used for heavy metal ion detection utilizing the produced liquid metal microdroplets as the working electrode. It is also demonstrated that a significant enhancement of the sensing performance is achieved by introducing acoustic streaming during the electrochemical experiments. The demonstrated technique can be used for developing liquid-metal-based systems for a wide range of applications.

1. Introduction

Micro- to nanosized droplets of gallium-based eutectic alloys such as EGaln (75% gallium, 25% indium) and Galinstan (68.5% gallium, 21.5% indium, 10% tin) have attracted considerable attention in the areas of 3D structure construction,^[1] reconfigurable/stretchable electronics,^[2] conductive composites,^[3] energy harvesting,^[4] electrochemical sensors,^[5] photocatalysts,^[5,6] inkjet printing,^[7] and nanomedicine.^[8] This is largely because such liquid metal alloys feature many useful properties including low melting point, high electrical and thermal conductivities, large surface tension, negligible vapor pressure, low viscosity, and the ability to form a passivating oxide layer in the presence of oxygen.^[9] Furthermore, these liquid metals do not suffer from the high toxicity issues as mercury does.

Several methods have been developed for producing micro- to nanosized liquid metal droplets including molding,^[10] flow-focusing,^[11] and sonication.^[2a,5-8,12] Using the molding method, liquid metal is spread onto a topographical mold patterned with cylindrical reservoirs to produce liquid metal microdroplets.^[10] While this method is simple, it is limited to producing large sphere diameters ($> 100 \mu\text{m}$), and the ability to mass produce such microdroplets would be time consuming. Another technique utilizes microfluidic flow-focusing devices, which can produce monodisperse liquid metal microdroplets.^[11] The size of the produced microdroplets is controlled by changing the shear rate or interfacial tension between the liquids.^[11a,d] Although the production rate of liquid metal microdroplets for flow-focusing method is significantly higher than that of molding method, producing droplets with sizes smaller than $50 \mu\text{m}$ is still challenging as smaller microchannels are required, or a high shear rate needs to be applied. Smaller microchannels or high shear rates induce very high pressure drops within the microchannel, causing instability for droplet production and can damage the microfluidic system.^[11d] Sonication of liquid metal in a nonsolvent is a simple and fast approach for producing a large amount of micro- to nanosized polydispersed droplets, with diameters ranging from less than a hundred nanometers to several micrometers.^[2a,5-8,12] Conventionally, a sonication bath or ultrasonication probe is used to break bulk liquid metal into smaller droplets. However, these sonication devices are bulky, and hence make it impossible to obtain integrated systems for miniaturized lab-on-a-chip applications. Moreover, in addition to sonication time and power, other less certain variables, such as the water level within the sonication bath tank, position of the liquid metal container inside the tank, as well as the position of the ultrasonication probe could also affect the size distribution of produced liquid metal microdroplets.

Precise control over the size of liquid metal microdroplets is essential to achieve the desired performance of the developed systems. It is also desirable that the droplet production system

is portable and versatile. Moreover, it would be better that additional transportation steps for the produced liquid metal droplets can be avoided to prevent contaminations. As such, a miniaturized and integrated system that allows on-chip production of micro- to nanosized liquid metal droplets with a controllable size distribution is ideal for the development of versatile lab-on-a-chip platforms for the applications in electronics, chemical/electrochemical sensors, and biomedical devices. In this work, we introduce an acoustic-based miniaturized system for on-chip production of EGaIn liquid-metal microdroplets with controllable size. The size distribution of liquid metal microdroplets is tuned by controlling the interfacial tension of the metal using either electrochemistry or electrocapillarity by applying an electrical potential to the liquid metal in the acoustic field. The utility of the produced liquid metal microdroplets is then demonstrated by using the same platform as an electrochemical sensor for Pb^{2+} ions detection. We demonstrate that the sensing performance is enhanced by inducing acoustic streaming within the buffer using the piezoelectric transducer to enhance the convective mass transport during the electrochemical experiments.

2. On-Chip Production of EGaIn Microdroplets with Controllable Size

Liquid metal microdroplets were produced from a bulk EGaIn droplet in the presence of acoustic wave-induced forces. The acoustic-based, on-chip liquid metal microdroplet production system is schematically shown in Figure 1A. The system consists of a piezoelectric transducer disk, which is bonded onto a thin glass slide ($22 \text{ mm} \times 40 \text{ mm} \times 100 \text{ }\mu\text{m}$) using epoxy glue. Owing to several advantages of piezoelectric transducer disks including low cost, small size and relatively large power output, they have been integrated into microfluidic platforms to generate acoustic waves, which are used to induce oscillations in trapped gas bubbles, or sharp edge microstructures built on the microchannel walls.^[13,14] The thin glass slide is placed on top of a polydimethylsiloxane (PDMS) post ($5 \times 5 \times 5 \text{ mm}$) to allow for maximum vibration. A polymethylmethacrylate (PMMA) well ($8 \times 8 \times 6 \text{ mm}$ with 1 mm wall thickness) with an Au/Cr coated thin glass ($12 \text{ mm} \times 12 \text{ mm} \times 100 \text{ }\mu\text{m}$) as the bottom is placed next to the transducer via double-sided tape, which allows the PMMA well to be disposable simply by detaching it from the tape using acetone. A piece of copper tape ($8 \text{ mm} \times 8 \text{ mm} \times 30 \text{ }\mu\text{m}$) is placed onto the bottom of the PMMA well to function as the working electrode. The entire system is placed onto a thick glass substrate ($25 \times 75 \times 1 \text{ mm}$). The actual experimental setup is shown in S1 (Supporting Information). Figure 1B shows the assembled schematics for the experimental setup, and Figure 2C,D show the detailed dimensions of the systems.

Our experimental results show that the production of EGaIn microdroplets is most efficient when the PMMA well is rotated by an angle of 45° with respect to the thin glass slide (see Figure 1C). This is probably because a localized high acoustic pressure region can be formed at the corner of the well nearest to the transducer. A $10 \text{ }\mu\text{L}$ EGaIn droplet is injected into the PMMA well and the well is filled with $350 \text{ }\mu\text{L}$ 0.1% (v/v) acetic acid solution (Figure 1B). Acetic acid provides ions for conducting electrical current and more importantly, it can later be removed by evaporation and thus it will not affect the characterization and electrochemical sensing experiments. A copper wire is placed into the

acetic acid solution and a potential is applied between the Au/Cr-coated glass and the copper wire to reduce or oxidize the EGaIn droplet (Figure 1B).

Production of EGaIn microdroplets can be achieved when the piezoelectric transducer is activated by signals with frequencies ranging from 6.8 to 8.2 kHz. Figure 2A–C show snapshots taken from a high-speed camera recording the production of EGaIn microdroplets using the developed platform. The piezoelectric transducer was activated with a 7 kHz, 175 V_{p-p} sinusoidal signal. The surface of the liquid metal droplet is oxidized in the acetic acid solution and a thin layer of gallium oxide skin is formed.^[9a] Such an oxide skin mechanically stabilizes the liquid metal in a nonspherical shape before the transducer is activated (Figure 2A). Interestingly, after activating the transducer, the EGaIn droplet transforms into a more spherical shape and at the same time dynamically forming symmetrical protrusions on the periphery of the droplet (Figure 2B). We believe that this is due to the presence of acoustic fields inside the PMMA well, which causes the droplet to vibrate. The vibration contains multiple eigenmodes. The oscillating shear forces within the PMMA well cause the non-Newtonian liquid to flow, fracturing and separating the thin oxide skin protecting the liquid metal.^[12] As a result, the large liquid metal droplet becomes unstable and starts to break into micro-sized droplets at the place close to the corner next to the transducer ≈ 0.5 s after transducer activation (Figure 2C). This microdroplet production process is also clearly shown in movie S1 (Supporting Information).

Scanning electron microscopy (SEM) images were taken for the microdroplets produced at different frequencies, as shown in S2 (Supporting Information). We find that the average size of the microdroplets produced at different frequencies is similar (40–50 μm in diameter) when the transducer is activated with a 175 V_{p-p} signal, as shown in Figure 2D. However, the time required to totally break the big droplet to microdroplets varies for different frequencies, with the minimum time observed when the applied frequency is around 7 kHz (Figure 2D). Additionally, we find that the size of the produced microdroplets slightly increases when the transducer is activated with smaller voltages, as shown in Figure 2E (the corresponding SEM images are given in S3, Supporting Information). Therefore, a 7 kHz, 175 V_{p-p} sinusoidal signal was chosen for the rest of the experiments for producing microdroplets unless specified otherwise.

The operating frequency in our experiments is in the range of 6.7 to 8.2 kHz. Since the speed of sound in glass is around 4540 m s⁻¹, the wavelength of the acoustic wave ranges from 670 to 550 mm, which is much larger than the size of the thin glass slide used in this work (22 mm \times 40 mm \times 100 μm). We do realize that since we use hard materials (with large acoustic impedance) such as PMMA, there would be reflections occurring at the channel walls. For this reason we calculated the natural frequency f_{nat} of our PMMA well filled with water using the equation $f_{\text{nat}} = 0.5c_w[(n_x/w)^2 + (n_y/l)^2 + (n_z/h)^2]^{0.5}$, where c_w is the speed of sound in water, $n_{x/y/z}$ are the mode numbers (1, 2, 3...) in the space elements, and w , l , h are the width, length, and height of the PMMA well, respectively. Based on our calculations, the minimum resonant frequency is around 90 kHz, which is much larger than our operating frequency. Thus, we believe that we do not set up any strong resonances and that no standing waves exist inside the PMMA well.

Breaking of the bulk EGaIn droplet into microdroplets occurs owing to the competition between destructive (shear forces) and cohesive (surface tension) forces on the liquid interface. The capillary number is a ratio of viscous forces to interfacial forces and is calculated as $Ca = \mu V/\gamma$, where μ and V are the viscosity and characteristic velocity of the acidic acid solution, respectively, and γ is the interfacial tension between EGaIn and therefore acetic acid solution. It is known that the size of microdroplets produced varies inversely with the capillary number.^[11c,d] We hypothesize that changing the interfacial tension of liquid metal during the acoustic activation process allows us to control the capillary number accordingly, and thus leads to the production of EGaIn microdroplets with different size distributions. The interfacial tension can be altered using either the electrochemistry or electrocapillarity approach. Electrochemically, the application of an oxidative bias to the liquid metal causes the formation of an oxide layer on the surface. Such oxide skin acts as a surfactant and lowers the interfacial tension of EGaIn.^[15] On the other hand, the application of a reducing bias induces charge accumulation at the metal–solution interface that reduces interfacial tension via electrocapillarity.^[15] Using this principle, it has been recently demonstrated that decreasing the size of liquid metal microdroplets produced in a microfluidic flow-focusing system can be achieved by changing the surface tension of liquid metal using oxidative or reducing bias.^[11d]

To prove the aforementioned hypothesis, we connected the liquid metal droplet to the anode via the Au/Cr-coated thin glass while connecting the acetic acid solution to the cathode through a copper wire (Figure 1B). It is known that a native oxide layer is formed after placing the EGaIn droplet into the solution, therefore, a -10 V reducing potential was first applied to the droplet for 5 s to electrochemically remove the native oxide layer. This procedure is necessary since the thickness of the native oxide layer for each EGaIn droplet could be different, and such difference affects the size distribution of the produced microdroplets. The transducer was activated 10 s after removing the native oxide layer while reducing/oxidative voltages ranging from -5 to 30 V were applied to the EGaIn droplet. Figure 3A shows the size distribution for the produced EGaIn microdroplets and their corresponding SEM images in the absence and presence of DC voltage upon activating the transducer with a 7 kHz, 175 V_{p-p} sinusoidal signal for 1 min. In the absence of DC voltage (0 V), the size of the produced microdroplets is widely distributed, ranging from 10 to 80 μm with an average diameter of ≈ 43 μm .

Interestingly, in the presence of a -5 V reducing potential (with the measured electrical current of ≈ 288 μA) while activating the piezoelectric transducer, the size distribution of EGaIn microdroplets shifted towards larger droplets to an average diameter of ≈ 61 μm (Figure 3A). Such a distribution shift can be attributed to the increased interfacial tension caused by the continuous electrochemical removal of the native oxide layer during the experiment. We found that no production of microdroplets was observed when the reducing voltage was increased to -10 V. This is due to the fact that the oxide layer was totally removed and merging of EGaIn microdroplets occurred.

Upon the application of a 5 V oxidative voltage (with the measured electrical current of ≈ 273 μA), the average diameter of produced EGaIn microdroplets decreases to ≈ 22 μm , and decreases further to ≈ 14 μm in response to 10 V, which is approximately a third of the size

of those produced at 0 V (Figure 3A). This indicates that the formation of the oxide layer significantly lowers the interfacial tension between EGaIn and the acetic acid solution, which makes it possible to produce smaller EGaIn microdroplets without increasing the activating power of the transducer. However, further increasing the oxidative voltage to 15 V and eventually to 30 V causes the size distribution of EGaIn microdroplets to shift towards larger droplets with average diameters above 30 μm , and the obtained microdroplets became less spherical in shape (in this case the diameter of a microdroplet is calculated by averaging the major and minor axis of the droplet). The diameter distributions of the microdroplets for the cases when 20 and 25 V oxidative voltages are applied are given in S4 (Supporting Information). Figure 3B summarizes the variations of the diameter of EGaIn microdroplets with respect to the applied reducing/oxidative voltage. The inset of Figure 3B shows that elongating the activating time of the transducer has negligible effect on the size of microdroplets.

In order to understand the obtained trend for the size distributions at different DC voltages (Figure 3B), SEM images were taken to show the surfaces of the microdroplets, as shown in Figure 3C–F. We can see that the surface of the microdroplet is relatively smooth when a -5 V reducing voltage is applied (Figure 3C) compared to the case when no voltage is applied (Figure 3D), indicating that such reducing voltage is able to electrochemically remove the native oxide layer on the surface of EGaIn and increase the interfacial tension, thus leading to the production of larger microdroplets. When a 10 V oxidative voltage is applied, the surface of EGaIn becomes more oxidized and less smooth (Figure 3E), and such an oxide layer may significantly lower the interfacial tension of EGaIn, allowing the production of smaller microdroplets. Interestingly, further increasing the oxidative voltage causes the formation of a thick and solid oxide layer on the surface of EGaIn (Figure 3F), and such a thick oxide skin prevents the oscillating shear force from breaking down the big droplet to smaller ones, causing the increased size of produced microdroplets.

We demonstrate that the developed system is able to achieve on-chip production of liquid metal microdroplets from bulk EGaIn in the presence of acoustic-induced forces. We also present that by applying an electrical potential to the liquid metal, both electrochemistry and electrocapillarity can be used to vary the size of produced microdroplets by controlling the interfacial tension of the metal. This ability is useful for making integrated on-chip liquid-metal-based electrochemical sensing devices, which will be demonstrated in the next section.

3. Enhancing Heavy Metal Ion Sensing Performance via Acoustic Waves

Like the conventionally used liquid metal mercury, gallium-based eutectic liquid metal alloys including Galinstan and EGaIn can accumulate different heavy metal ions at the surface.^[16] It has been previously reported that a hanging Galinstan droplet electrode (HGDE) can be employed in the voltammetric analysis of heavy metal ions such as Pb^{2+} ,^[16] and the micro- to nanosized liquid metal/metal oxide spherical structures are able to increase the sensitivity further as they have a large surface to volume ratio.^[5] In our system, the PMMA well can be used as an electrochemical sensing platform simply by placing a PMMA cap with inserted Ag/AgCl reference and graphite auxiliary electrodes, as shown in Figure

4A (see S5, Supporting Information for actual experimental setup). In stationary electrochemical detection systems, the reaction occurs near the electrodes and creates a diffusion layer, such a layer limits the current flow and hence the threshold of detection. In order to improve the sensitivity, convective enhancement of mass transfer is required to break down the diffusion barriers at the electrode interface.^[17] In our developed system, we have demonstrated the capability of the acoustic-wave-induced forces for producing microdroplets of EGaIn. We also hypothesize that such acoustic waves are able to induce acoustic streaming within the PMMA well to significantly enhance the convective mass transport during electrochemical sensing, hence leading to an increase in sensitivity.

In order to prove the aforementioned hypothesis, the developed system was used for Pb²⁺ heavy metal ion sensing. In this system, a 10 μ L single EGaIn droplet or produced EGaIn microdroplets were immobilized on a copper tape substrate and used as the working electrode. The EGaIn microdroplet working electrode was obtained by placing the thin glass slide onto an 80 °C hot plate to evaporate the acetic acid solution after the application of acoustic waves. The EGaIn microdroplets were patterned tightly together after evaporation and no disturbance of the structure was observed after adding electrochemical sensing buffer in the PMMA well. In order to show the capability of the acoustic waves for producing vortices within the PMMA well to enhance the convective mass transfer, numerical simulations were conducted to study the pressure distribution within the PMMA well after activating the transducer by an 8 kHz AC signal, as shown in Figure 4B–D. A simplified numerical model was used to observe the acoustic fields inside the PMMA well without the presence of EGaIn droplets and electrodes. The details of the numerical model are provided in S6 (Supporting Information). Figure 4C,D show the pressure distribution for the cross-sectional areas given in the red and black boxes, respectively. High acoustic pressure is produced at the corner next to the transducer. Such pressure distribution is expected to induce two symmetrical vortices within the PMMA well, and this is experimentally proved as shown in Figure S6C and Movie S2 (Supporting Information). Polystyrene microparticles with a diameter of 15 μ m were used to show the trajectories of the induced vortices. The full resolution of the acoustic streaming response demands a mesh resolution on the order of viscous boundary layer width. For our device, owing to the large mismatch between the device dimensions (with substrate length of the order of 1 cm) and the characteristic length scales of the second-order solution (the viscous boundary layer width: 1–10 μ m), even a fully resolved 2D simulation of the full system is computationally expensive. Nonetheless a 2D simulation of the second-order fields provides valuable qualitative insights into the acoustic streaming flow formed inside the PMMA well, which is shown in Figure S6D,E (Supporting Information).

270 μ L ammonium acetate buffer containing Pb²⁺ ions with a concentration of 10 ppm was added to the PMMA well, and differential pulse anodic stripping voltammograms of Pb²⁺ were performed with a single EGaIn droplet used as the working electrode. In the beginning, a cathodic potential of –0.8 V was applied for 180 s in the absence of acoustic waves to preconcentrate metallic lead (reduce Pb²⁺ to Pb⁰) into the EGaIn liquid metal. The differential pulse voltammograms (DPVs) were then performed from –0.8 to –0.4 V, as shown in Figure 4E. The oxidation peak potential for Pb⁰ stripping is found to be at around –0.62 V. Interestingly, an increase in the oxidation peak is observed when the transducer is

activated by 20 V_{p-p} sinusoidal signals with frequencies ranging from 7 to 9 kHz during the preconcentration step, which is shown clearly in the inset of Figure 4E. The amplitude of the oxidation current peak reaches its largest value at 8 kHz, which is ≈3 times higher than measurements when acoustic waves are absent. The currents at the preconcentration step were recorded with different transducer activating frequencies using the current–time amperometry technique, as shown in S7 (Supporting Information). It can be seen that the current wave is smooth when acoustic waves are absent. However, the magnitudes of the currents increase and become unstable when acoustic waves are applied, with the largest current obtained at 8 kHz, which is in line with the DPVs obtained in Figure 4E, indicating the effect of the enhanced convective mass transfer due to the induced acoustic streaming within the PMMA well.

Next, we obtained DPVs using EGaIn microdroplets as the working electrode in the absence or presence of acoustic waves, as shown in Figure 4F. In this case, EGaIn microdroplets obtained with an oxidative voltage of 5 V were used. Interestingly, although the size of microdroplets is the minimum when a 10 V oxidative voltage is applied (Figure 3B), the maximum amplitude of the oxidation current peak was obtained for the microdroplets produced with a 5 V oxidative voltage, as shown in S8 (Supporting Information). This could be due to the fact that the thick oxide layer formed on microdroplets produced at higher oxidative voltages may prevent the accumulation of Pb²⁺ ions on the surface during the preconcentration step. Similar to the DPVs obtained with a single EGaIn droplet, the presence of acoustic waves leads to a significant increase in sensitivity (≈8 times), and the amplitude of the oxidation current peak is the largest at 8 kHz. The diameter of a 10 μL EGaIn droplet is ≈1.34 mm and the calculated surface area of the droplet is ≈22.45 mm². Taking the average size (≈22 μm in diameter) of the EGaIn microdroplets produced with a 5 V oxidative potential (see Figure 3B), the total surface area increases to ≈2700 mm² after breaking the big droplet into microdroplets, which is ≈120 times larger than that of a single droplet. However, we only observed a ≈6 times enhancement of the sensing performance using the microdroplets at 8 kHz compared to the case where a single EGaIn droplet is used. This could be due to the fact that the oxide layer formed on the surface of microdroplets compromises the electrical path between the microdroplets and also prevents the accumulation of Pb²⁺ ions on their surface during the preconcentration step.

Additionally, we investigated the effect of streaming speed on the sensitivity of Pb²⁺ ions by changing the V_{p-p} of the activating signal for the transducer, as shown in Figure 4G. The amplitude of the oxidation current peak increases when a larger V_{p-p} is applied, reaching its maximum at an activating voltage of 20 V_{p-p}. Further increasing the voltage to 25 V lowers the oxidation current peak; this could be attributed to the fact that larger transducer signals could compromise the integrity of the patterned EGaIn microdroplet structure, leading to a weaker sensing performance.

It has been previously reported that liquid metal marbles, which are liquid metal droplets coated with layers of nanoparticles, are capable of achieving higher sensitivity for heavy metal ions detection in comparison to their non-coated counterparts^[18] This enhancement is attributed to factors including the generation of localized electric fields at the electrolyte/nanoparticle/liquid metal triple phase boundary, interaction between heavy metal ions and

the nanoparticles due to the existence of partial charges on the surface of nanoparticles, as well as the enlarged surface area produced by the nanoparticles.^[5,18,19] It is expected that in the presence of acoustic wave induced streaming, the developed system is able to achieve on-chip production of uniformly coated microsized liquid metal marbles (mLMMs) and such mLMMs can be used for further enhancing the sensitivity of Pb^{2+} ion detection.

In this study, WO_3 nanoparticles (≈ 100 nm diameter) were chosen as it has been previously reported that the WO_3 nanoparticles coated liquid metal marbles provide much higher sensitivity for heavy metal ion detection compared to the results obtained using uncoated Galinstan droplets or droplets coated with other nanoparticles.^[18] To produce such mLMMs with different coating densities, 50 to 200 mg of WO_3 nanoparticles were added into 10 mL 0.1% acetic acid solution to produce WO_3 suspensions with concentrations ranging from 5 to 20 mg mL^{-1} . Next, 350 μL of the prepared WO_3 nanoparticle suspension was added to the PMMA well together with a 10 μL EGaIn droplet, and EGaIn microdroplets were produced and mixed with the nanoparticles by activating the transducer as previously described with the presence of a 5 V oxidative voltage. Finally, the mLMMs were obtained by placing the thin glass slide onto an 80 °C hot plate to evaporate the acetic acid solution. Figure 5A shows the surface morphology of the produced mLMMs obtained by using WO_3 suspension with a concentration of 10 mg mL^{-1} . It can be seen that the EGaIn microdroplets are uniformly coated with multilayers of WO_3 nanoparticles.

Similarly, differential pulse anodic stripping voltammograms of Pb^{2+} were performed using the mLMMs as the working electrode. Figure 5B presents the DPVs obtained by mLMMs produced from WO_3 nanoparticle suspensions with different concentrations. The transducer was activated by an 8 kHz, 20 $V_{\text{p-p}}$ sinusoidal signal during the preconcentration step. The highest sensitivity was achieved when the concentration of the nanoparticle suspension is set at 10 mg mL^{-1} , which is $\approx 40\%$ higher than the case without WO_3 nanoparticle coating.

Figure 5C shows the DPVs measured as a function of Pb^{2+} concentration. The Pb^{2+} ions detection limit of the system is found to be 500 ppb. The amplitude of the oxidation current peak has a linear response to the ion concentrations, as shown in Figure 5D. It should be noted that the limit of detection is higher than the results obtained in the previous study (100 ppb) where micro- to nanosized Galinstan droplets were used.^[5] This is likely due to the smaller size (< 5 μm diameter) of liquid metal microdroplets, which were obtained using a high power sonication bath, and in turn a larger surface area was available to accommodate more WO_3 nanoparticles.^[5] The overall comparison for the DPVs obtained with a single EGaIn droplet, EGaIn microdroplets and mLMMs with or without acoustic waves is summarized in Figure S8B (Supporting Information). It can be seen that a ≈ 22 times enhancement of sensitivity for Pb^{2+} detection is achieved when mLMMs are used in the presence of acoustic waves compared to the case when a single EGaIn droplet is used in the absence of acoustic waves.

4. Conclusion

In summary, we developed a versatile miniaturized system for on-chip mass production of EGaIn liquid metal microdroplets with controllable size using acoustic-wave-induced forces.

The size of the produced EGaIn microdroplets is controlled by applying voltages to change the surface tension of the liquid metal using either electrochemistry or electrocapillarity when acoustic field is applied. This method can change the average diameter of liquid-metal microdroplets by a factor of ≈ 4 , simply by varying the magnitude of the applied oxidative voltage. Most importantly, our system avoids the use of conventional bulky sonication baths or probes which are less portable, expensive, and complex, having many concerning variables for producing microdroplets with controllable sizes. The versatility of the system and the utility of the produced liquid metal microdroplets are then demonstrated by using the same platform as an electrochemical sensor for heavy metal ion detection. These liquid metal microdroplets together with WO_3 nanoparticles are used to form microsized liquid metal marbles for establishing a highly sensitive electrochemical sensing platform. We demonstrate that in addition to generating the acoustic forces required for producing EGaIn microdroplets, the transducer in the platform can also be used for inducing acoustic streaming within the PMMA well when lowering the magnitude of the activating voltage. Such streaming enhances the convective mass transport during the preconcentration step for Pb^{2+} ions, leading to a significant enhancement of sensitivity for Pb^{2+} ion detection. Altogether, the developed system provides strong prospects for the development of integrated liquid metal microdroplet enabled applications in colloidal inks, composites,^[3] electrochemical sensors,^[5] photocatalysts,^[5,6] or nanomedicine.^[8] More importantly, liquid metal microdroplets can be assembled into 3D structures to develop electronic devices such as antennas,^[2] electrodes,^[1b] loudspeakers,^[20] capacitors,^[21] and UV sensors.^[22] Furthermore, it is also worth exploring the possibility of using surface acoustic waves enabled microfluidic platforms to further miniaturize the system for on-chip production and manipulation of liquid metal microdroplets.^[23,24]

5. Experimental Section

Chemicals, Reagents, and Preparation:

EGaIn, acetic acid (>99%), ammonium acetate powder (>99%), lead (II) acetate 3-hydrate, and WO_3 nanoparticles (≈ 100 nm) were purchased from Sigma Aldrich, USA. 0.1% (v/v) acetic acid solution was prepared by adding 50 μL acetic acid into 49.95 mL DI water. WO_3 suspension was prepared by mixing 50 to 200 mg WO_3 nanoparticles with 10 mL 0.1% acetic acid solution to yield concentrations of 5 to 20 mg mL^{-1} . Then the WO_3 suspension was kept in a sonication bath for 20 min to prevent agglomeration.

Experimental Setup:

Acoustic waves were produced by a piezoelectric transducer disk (Murata Electronics, USA) with a diameter of 20 mm bonded to a thin glass slide (22 mm \times 40 mm \times 100 μm) driven by a function generator (Tektronix AFG 3011, USA). The platform was mounted on the stage of an inverted microscope (Nikon TE-2000U, USA). Formation of EGaIn was captured using a Photron SA4 fast camera connected to the microscope. SEM images were obtained using a Leo 1530 field emission scanning electron microscope (FESEM). The PMMA well (8 \times 8 \times 6 mm) with 1 mm wall thickness is obtained by cutting a 6 mm thick PMMA plate using a CO_2 laser cutter (Epilog Zing, USA), and the well is bonded to an Au/Cr (50/5 nm)

coated thin glass slide (1.2×1.2 mm) using epoxy glue. The numerical solution was conducted using the finite element software COMSOL Multiphysics 5.1.

Heavy Metal Ion Sensing:

The working electrode for Pb^{2+} ions detection was first prepared by wetting a copper tape with EGaIn. Then the liquid metal microdroplets or microsized liquid metal marbles were formed after activating the transducer and later on uniformly deposited onto the substrate by dehydrating the platform on a hotplate at $80\text{ }^{\circ}\text{C}$. All measurements were performed using a CH Instruments (CHI 830D, USA) electrochemical analyzer. The reference electrode was Ag/AgCl (aqueous 3 M KCl) and an inert graphite rod (2 mm diameter, Equalseal, USA) was used as the auxiliary electrode. For stripping voltammetry, 0.1 M acetate buffer solution was prepared by dissolving 3.35 g ammonium acetate into 50 mL DI water. The pH of the buffer was adjusted to 6.0 by adding acetic acid and measured using a microprocessor controlled pH meter. Lead ions (Pb^{2+}) were incorporated in the supporting electrolyte by dissolving lead (II) acetate 3-hydrate. Prior to every scan, a preconditioning step (180 s at -0.8 V) was applied. The voltammogram was recorded by applying a positive-going scan from -0.8 to -0.4 V with a step increment of 5 mV, amplitude of 80 mV, and pulse period of 0.2 s.

Supplementary Material

Refer to Web version on PubMed Central for supplementary material.

Acknowledgements

The authors gratefully acknowledge financial support from National Institutes of Health (GM112048 and EB019785), National Science Foundation (IIP-1534645 and IDBR-1455658), American Asthma Foundation (AAF) Scholar Award, and the Penn State Center for Nanoscale Science (MRSEC) under grant DMR-1420620. Components of this work were conducted at the Penn State node of the NSF-funded National Nanotechnology Infrastructure Network. The authors also acknowledge the Research Computing and Cyberinfrastructure Unit of Information Technology Services at The Pennsylvania State University for providing advanced computing resources and services that have contributed to the research results reported in this paper.

References

- [1] a). Ladd C, So JH, Muth J, Dickey MD, Adv. Mater 2013, 25, 5081; [PubMed: 23824583] b)Tang S-Y, Zhu J, Sivan V, Gol B, Soffe R, Zhang W, Mitchell A, Khoshmanesh K, Adv. Funct. Mater 2015, 25, 4445.
- [2] a). Lin Y, Cooper C, Wang M, Adams JJ, Genzer J, Dickey MD, Small 2015, 11, 6397; [PubMed: 26568095] b)Zheng Y, He Z-Z, Yang J, Liu J, Sci. Rep 2014, 4, 4588. [PubMed: 24699375]
- [3]. Fassler A, Majidi C, Adv. Mater 2015, 27, 1928. [PubMed: 25652091]
- [4]. Krupenkin T, Taylor JA, Nat. Commun 2011, 2, 448. [PubMed: 21863015]
- [5]. Zhang W, Ou JZ, Tang SY, Sivan V, Yao DD, Latham K, Khoshmanesh K, Mitchell A, O'Mullane AP, Kalantar-Zadeh K, Adv. Funct. Mater 2014, 24, 3799.
- [6] a). Zhang W, Naidu BS, Ou JZ, O'Mullane AP, Chrimes AF, Carey BJ, Wang Y, Tang S-Y, Sivan V, Mitchell A, ACS Appl. Mater. Interfaces 2015, 7, 1943; [PubMed: 25543876] b)O'Mullane AP, Chem. Commun 2015, 51, 14026.
- [7]. Boley JW, White EL, Kramer RK, Adv. Mater 2015, 27, 2355. [PubMed: 25728533]
- [8]. Lu Y, Hu Q, Lin Y, Pacardo DB, Wang C, Sun W, Ligler FS, Dickey MD, Gu Z, Nat. Commun 2015, 6, 10066. [PubMed: 26625944]
- [9] a). Dickey MD, ACS Appl. Mater. Interfaces 2014, 6, 18369; [PubMed: 25283244] b)Liu T, Sen P, Kim C-JC, J. Microelectromech. Syst 2012, 21, 443.

- [10]. Mohammed MG, Xenakis A, Dickey MD, *Metals* 2014, 4, 465.
- [11] a). Thelen J, Dickey MD, Ward T, *Lab Chip* 2012, 12, 3961; [PubMed: 22895484] Hutter T, Bauer WAC, Elliott SR, Huck WT, *Adv. Funct. Mater* 2012, 22, 2624;b)Gol B, Tovar-Lopez FJ, Kurdzinski ME, Tang S-Y, Petersen P, Mitchell A, Khoshmanesh K, *Lab Chip* 2015, 15, 2476; [PubMed: 25943915] c)Tang S-Y, Joshipura ID, Lin Y, Kalantar-Zadeh K, Mitchell A, Khoshmanesh K, Dickey MD, *Adv. Mater* 2015, 28, 604. [PubMed: 26601792]
- [12]. Hohman JN, Kim M, Wadsworth GA, Bednar HR, Jiang J, LeThai MA, Weiss PS, *Nano Lett* 2011, 11, 5104. [PubMed: 22023557]
- [13]. Ahmed D, Ozcelik A, Bojanala N, Nama N, Upadhyay A, Chen Y, Hanna-Rose W, Huang TJ, *Nat. Commun* 2016, 7, 11085. [PubMed: 27004764]
- [14]. Huang P-H, Ren L, Nama N, Li S, Li P, Yao X, Cuento RA, Wei C-H, Chen Y, Xie Y, Nawaz AA, Alevy YG, Holtzman MJ, McCoy JP, Levine SJ, Huang TJ, *Lab Chip* 2015, 15, 3125. [PubMed: 26082346]
- [15]. Khan MR, Eaker CB, Bowden EF, Dickey MD, *Proc. Natl. Acad. Sci* 2014, 111, 14047. [PubMed: 25228767]
- [16]. Surmann P, Zeyat H, *Anal. Bioanal. Chem* 2005, 383, 1009. [PubMed: 16228199]
- [17]. Klima J, *Ultrasonics* 2011, 51, 202. [PubMed: 20804997]
- [18]. Sivan V, Tang SY, O'Mullane AP, Petersen P, Eshtiaghi N, Kalantar-Zadeh K, Mitchell A, *Adv. Funct. Mater* 2013, 23, 144.
- [19]. Kosmulski M, *Chemical Properties of Material Surfaces*, Vol. 102, CRC press, New York 2001.
- [20]. Jin SW, Park J, Hong SY, Park H, Jeong YR, Park J, Lee S-S, Ha JS, *Sci. Rep* 2015, 5, 11695. [PubMed: 26181209]
- [21]. Fassler A, Majidi C, *Lab Chip* 2013, 13, 4442. [PubMed: 24067934]
- [22]. Yoon J, Hong SY, Lim Y, Lee S-J, Zi G, Ha JS, *Adv. Mater* 2014, 26, 6580. [PubMed: 25159006]
- [23]. Ding X, Li P, Lin S-CS, Stratton ZS, Nama N, Guo F, Slotcavage D, Mao X, Shi J, Costanzo F, Huang TJ, *Lab Chip* 2013, 13, 3626. [PubMed: 23900527]
- [24]. Li S, Ding X, Guo F, Chen Y, Lapsley M, Lin S-CS, Wang L, McCoy JP, Cameron C, Huang TJ, *Anal. Chem* 2013, 85, 5468. [PubMed: 23647057]

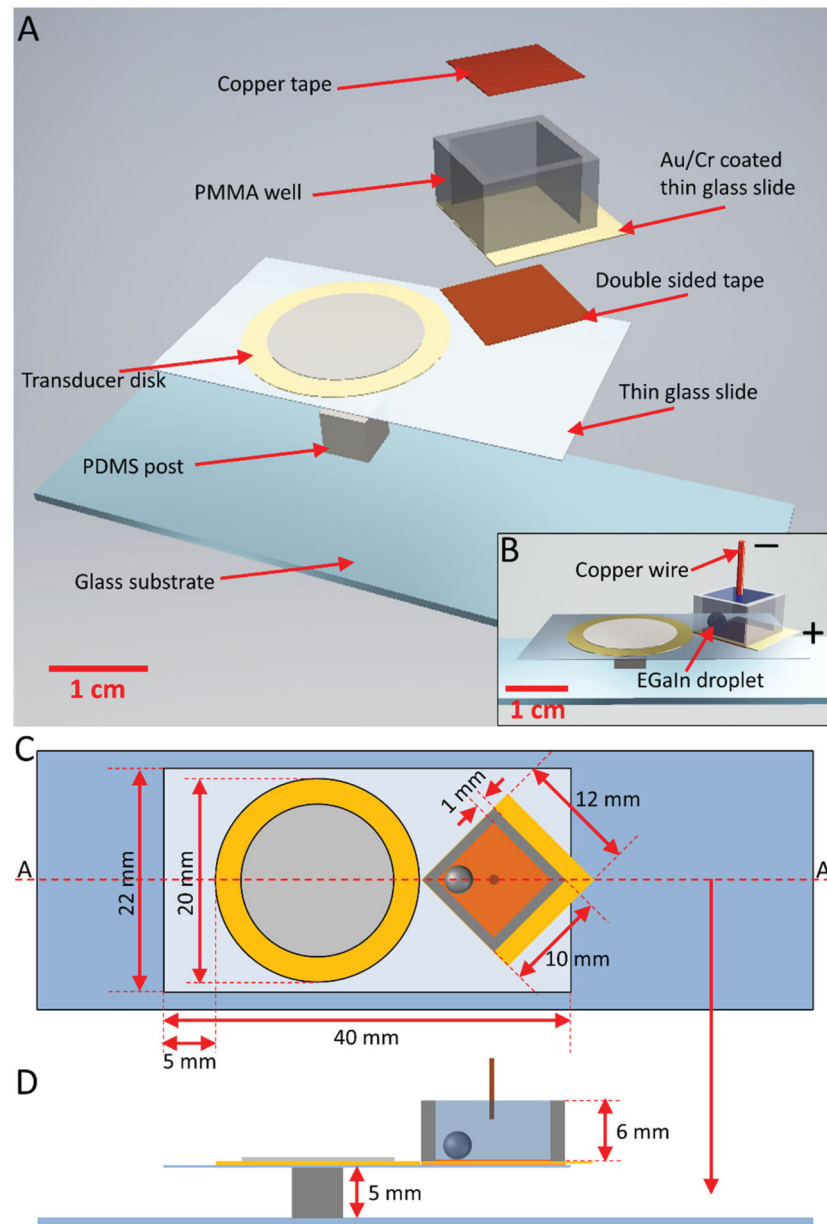


Figure 1. Schematics of the acoustic-based liquid metal microdroplet production platform. A) Exploded schematic. B) Assembled schematic with an EGaIn droplet and copper wire placed inside the PMMA well. C) Top view of the experimental setup. D) Cross-sectional view of the experimental setup along the line AA' in (C).

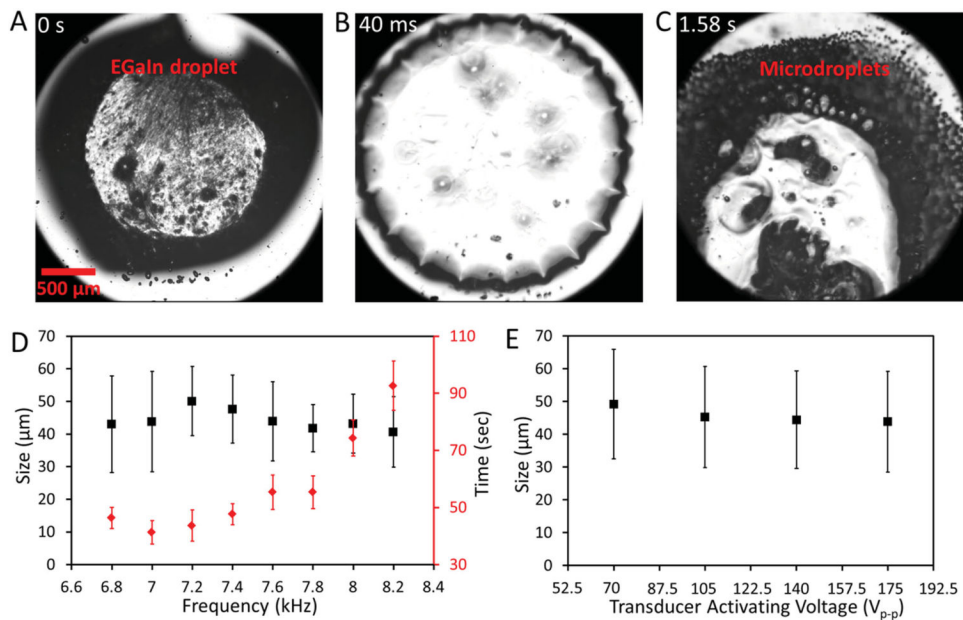


Figure 2. Production of EGaln microdroplets. Snapshot images showing the production of EGaln microdroplets from one single droplet after activating the piezoelectric transducer with a 7 kHz, 175 V_{p-p} sinusoidal signal at A) 0 s, B) 40 ms, and C) 1.58 s. D) Mean and standard deviation of the microdroplet diameter (black square), and time required for fully breaking a bulk droplet to microdroplets (red diamond) vs transducer activating frequency plot. The voltage applied to the transducer is set at 175 V_{p-p}. E) Mean and standard deviation of the microdroplet diameter vs voltage applied to the piezoelectric transducer. The frequency of the transducer is set at 7 kHz.

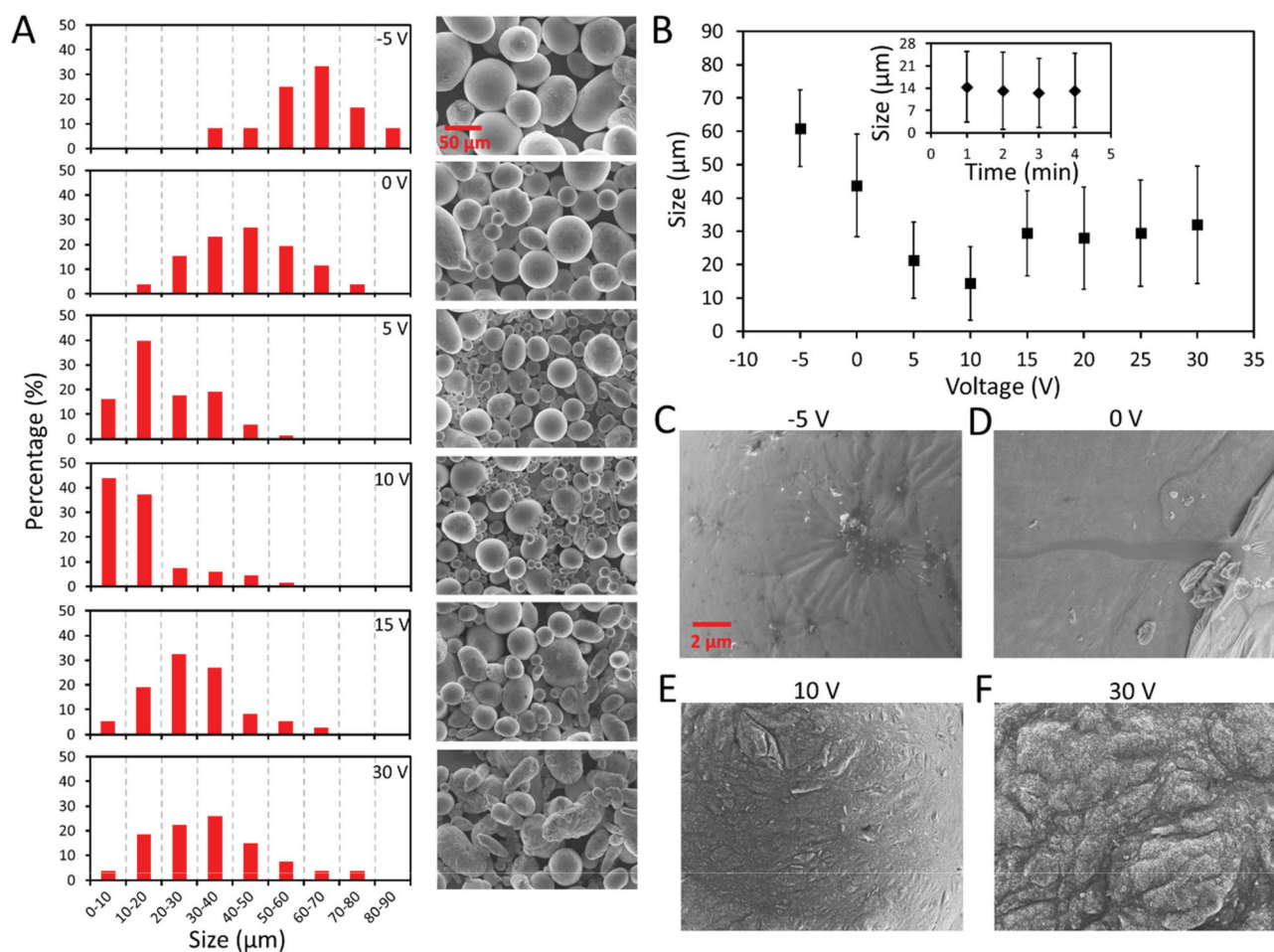


Figure 3.

Characterization of the produced EGaln microdroplets at different oxidative/reducing voltages. A) Size distribution of the EGaln microdroplets and their corresponding SEM images for microdroplets produced when DC voltages ranging from -5 to 30 V are applied to the EGaln droplet. B) Mean and standard deviation of the microdroplet diameter vs applied voltage plot. The inset shows the mean and standard deviation of the microdroplet diameter vs transducer activating time plot when an oxidative potential of 10 V is applied. SEM images for the surface of produced EGaln microdroplets when a voltage of C) -5 , D) 0 , E) 10 , and F) 30 V is applied to the EGaln droplet.

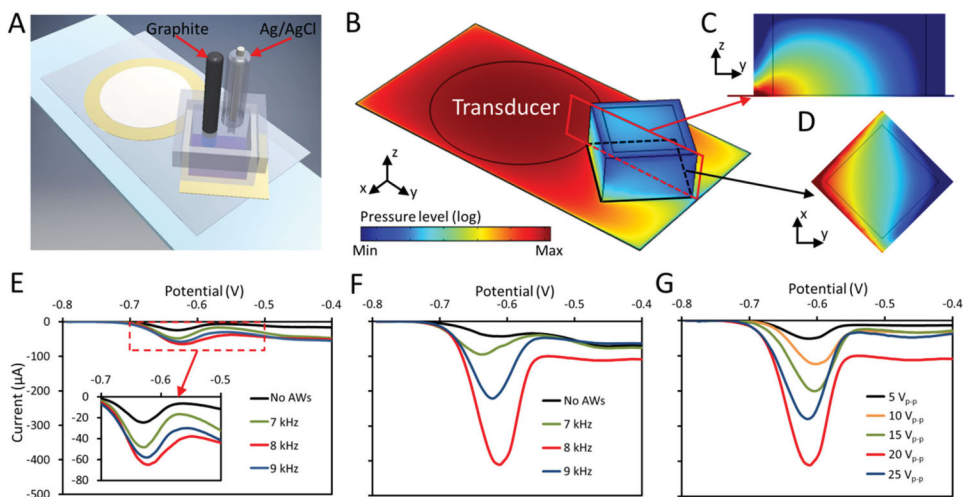


Figure 4. Pb^{2+} ion sensing using a single or microdroplet based EGaIn probe with or without acoustic waves. A) Schematic of the acoustic-based platform for electrochemical sensing of Pb^{2+} ions. B) Color plot for the distribution of the pressure field in the platform. Color plots of the pressure field distribution (blue minimum to red maximum) on the C) yz-plane (cross-sectional area given in the red box) and D) xy-plane (cross-sectional area given in the black box) in the PMMA well. E) DPVs for Pb^{2+} ion sensing recorded using a $10\ \mu\text{L}$ single EGaIn droplet without or with acoustic waves at different frequencies. The inset shows a magnified plot of the response. F) DPVs recorded using EGaIn microdroplets produced with a $5\ \text{V}$ oxidative voltage without or with acoustic waves at different frequencies. G) DPVs recorded using EGaIn microdroplets when different activating voltages are applied to the transducer. The frequency of the signals is set at $8\ \text{kHz}$.

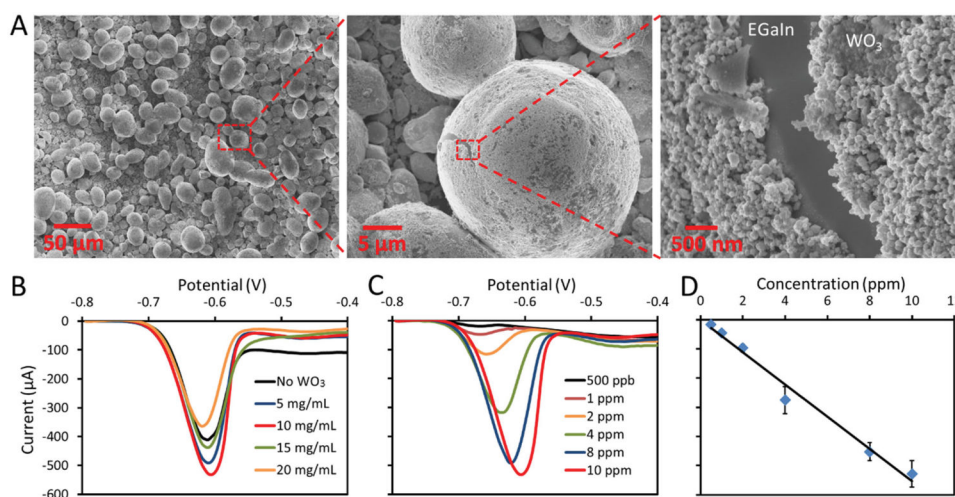


Figure 5. Pb²⁺ ion sensing using WO₃ nanoparticles coated microsized EGaIn liquid metal marbles. A) SEM images for the WO₃ nanoparticles coated mLMs obtained when WO₃ suspension with a concentration of 10 mg mL⁻¹ is used. B) DPVs recorded using mLMs produced with different WO₃ nanoparticle suspension concentrations. C) DPVs for increasing concentrations of Pb²⁺ recorded with mLMs obtained using WO₃ suspension with a concentration of 10 mg mL⁻¹. D) Pb²⁺ concentration vs amplitude of the oxidation current peak plot.